



# Stereomodulating effect of remote groups on the NADH-mimetic reduction of alkyl aroylformates with 1,4-dihyronicotinamide- $\beta$ -lactam amides

Jesus M. Aizpurua\*, Claudio Palomo, Raluca M. Fratila, Pablo Ferrón, José I. Miranda

Departamento de Química Orgánica-I, Universidad del País Vasco, Joxe Mari Korta R&D Center, Avda. Tolosa-72, 20018 San Sebastián, Spain

## ARTICLE INFO

### Article history:

Received 12 January 2010

Received in revised form 18 February 2010

Accepted 22 February 2010

Available online 25 February 2010

### Keywords:

NADH

$\beta$ -Lactams

DFT calculations

Enantioselective reduction

## ABSTRACT

Conformationally restricted NADH peptidomimetics **4a–e**, characterized by the presence of a (1,4-dihyronicotinamide)-( $\beta$ -lactam) moiety, have been synthesized and used to study the  $Mg^{2+}$  cation-promoted asymmetric reduction of alkyl aroylformates in acetonitrile. Increasing the bulkiness of peripheral substituents at the nitrogen atom of the  $\beta$ -lactam ring, at the 1,4-dihyronicotinamide moiety, or at the aroylformate ester group, was found to cause weak but clearly detectable variations of the enantiomeric excess of the reaction. A rationale for these observations was consistent with a chelated  $NADH/Mg^{2+}/ArCOCO_2R^3$  ternary complex model, according to DFT calculations computed at a B3LYP/6-31G\* theory level.

© 2010 Elsevier Ltd. All rights reserved.

## 1. Introduction

Nicotinamide adenine dinucleotide ( $NAD^+$ ) and its reduced form NADH are cofactors of L-lactate dehydrogenase, which is involved in the enantioselective reduction of pyruvate during anaerobic glycolysis. As NADH binds to the enzyme, different conformational changes occur at the active site,<sup>1</sup> resulting in the controlled orientation of the substrate approach and in the stereoselective transfer of one of the diastereotopic hydrogen atoms in NADH to the prochiral pyruvate.<sup>2</sup> The 1,4-dihyronicotinamide moiety acts in NADH as an inherently reactive and recyclable center for the catalytic activity.<sup>3</sup> Thus, many organic and bioorganic chemists have been challenged to mimic the activity of the  $NAD^+$ /NADH redox system. Since the first asymmetric reduction using an NADH mimic reported by Ohno<sup>4</sup> in 1975 a large number of approaches to NADH mimicking have been made.<sup>5</sup> Conventional strategies to design an efficient biomimetic system include the synthesis of 1,4-dihydropyridines with a chiral center at C4<sup>6</sup> and/or chiral side arms on the carbamoyl group.<sup>7–10</sup> Generally, the nonenzymatic reduction of activated carbonyl compounds (e.g.,  $\alpha$ -keto esters) is achieved in the presence of a suitable divalent metal ion (most often  $Mg^{2+}$  and  $Zn^{2+}$ ), which plays a fundamental role in the activation and stereodirection of the hydride transfer mechanism.<sup>11</sup> Within this context, 1,4-dihyronicotinamide peptides **1**<sup>12,13</sup> (Fig. 1)

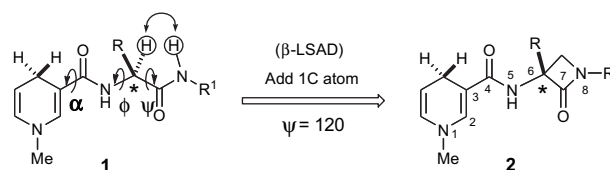


**Figure 1.** The ‘ $\beta$ -Lactam Scaffold-Assisted Design’ ( $\beta$ -LSAD) approach to NADH models: formal insertion in the native peptide of one single carbon atom ( $C\alpha-H+N \rightarrow C\alpha-CH_2-N$ ) provides pseudopeptides **2** rigidified around the  $\psi$  ( $\approx 120^\circ$ ) torsion angle. Definition of dihedral angles:  $\alpha$ : ( $C^2-C^3-C^4-N^5$ ),  $\phi$ : ( $C^4-N^5-C^6-C^7$ ),  $\psi$ : ( $N^5-C^6-C^7-N^8$ ).

represent, not only interesting artificial models to mimic the chiral field of enzymatic NADH reductions, but also excellent probes to conduct mechanistic and computational studies on the origin of the stereoselectivity of  $Mg^{2+}$ -promoted nonenzymatic reactions. Since they are able to form strongly chelated intermediates with  $Mg^{2+}$  cation, they can be used to further understand the architecture of the  $NADH/Mg^{2+}/ArCOCO_2R$  ternary complexes and the subsequent transition states leading to the nonracemic reduction products.

Recently, we have introduced the puckering-free  $\beta$ -lactam NADH mimetics **2** to decrease the flexibility around the chelated reaction intermediates in these reduction reactions.<sup>14</sup> Inspired in the Freidinger’s inter-residual  $C\alpha-N$  bridging,<sup>15</sup> 1,4-dihyronicotinamide- $\beta$ -lactam peptides **2** were designed to have simultaneously a minimal scaffold and a maximal rigid constraint issued from the ‘ $\beta$ -LSAD’ principle.<sup>16</sup> This enabled a more accurate interpretation of computational calculations by minimizing the

\* Corresponding author. Tel.: +34 943 015383; fax: +34 943 015959.

E-mail address: [jesusmaria.aizpurua@ehu.es](mailto:jesusmaria.aizpurua@ehu.es) (J.M. Aizpurua).

energy contributions arising from the conformational mobility around the  $\varphi$  and  $\psi$  dihedral angles. Owing to this particular design, the transition state TS-I (Fig. 2) could be characterized at a B3LYP/6-31G\* computation level as the preferred pathway for the reduction of methyl benzoylformate to the (*S*)-methyl mandelate major product.<sup>14</sup> The intrinsic stereodirecting effect of the  $\beta$ -lactam ring was also studied experimentally from *N*-[bis(trimethylsilyl)methyl]- $\beta$ -lactams **3** and it was shown to be superior to the nonbridged NADH peptides **1**. Accordingly, it was found that the enantiomeric excess of the reduction increased with the bulkiness of the  $\alpha$ -substituent attached to the stereogenic center of the  $\beta$ -lactam ring.

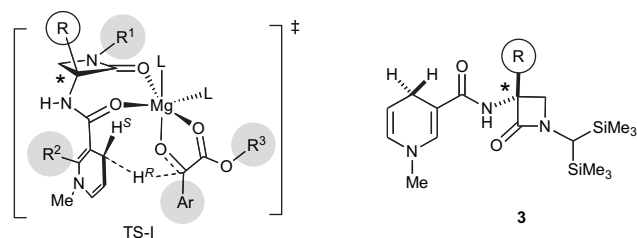


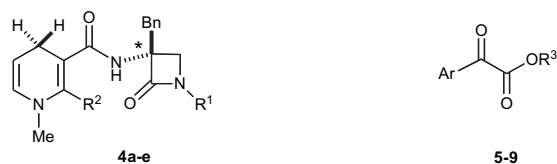
**Figure 2.** Lower-energy structure of the NADH/Mg<sup>2+</sup>/ArCOCO<sub>2</sub>R<sup>3</sup> ternary transition state predicted by B3LYP/6-31G\* computation for the enantioselective reduction of alkyl aroylformates with the  $\beta$ -lactam mimetics **3**. Peripheral groups are highlighted in gray color.

Despite this general stereodirecting trend, our chelating model should also explain the yet unknown modulation of the enantiomeric excess by peripheral groups distant from the asymmetric stereocenter (e.g., R<sup>1</sup>, R<sup>2</sup>, R<sup>3</sup>, and Ar in Fig. 2). Herein we report our investigation concerning the synthesis of diversely substituted enantiopure 1,4-dihydronicotinamide- $\beta$ -lactam mimetics **4** (see below) and the experimental and computational exploration of their reactivity as enantioselective reducing agents of various alkyl aroylformate esters **5–9**. Our new experimental results are reflected in the computations, confirming the previously proposed chelated ternary entity TS-I as a plausible model to account for the stereochemical behavior observed in these nonenzymatic NADH reduction reactions.

## 2. Results and discussion

### 2.1. Synthesis of NADH peptide $\beta$ -lactam models

The 1,4-dihydronicotinamides **4a–e** bearing R<sup>1</sup> and R<sup>2</sup> groups of different size (Fig. 3) were synthesized to be used as constrained NADH peptide models.  $\beta$ -Lactams **4a–c** were readily accessible through the total or partial desilylation of the large

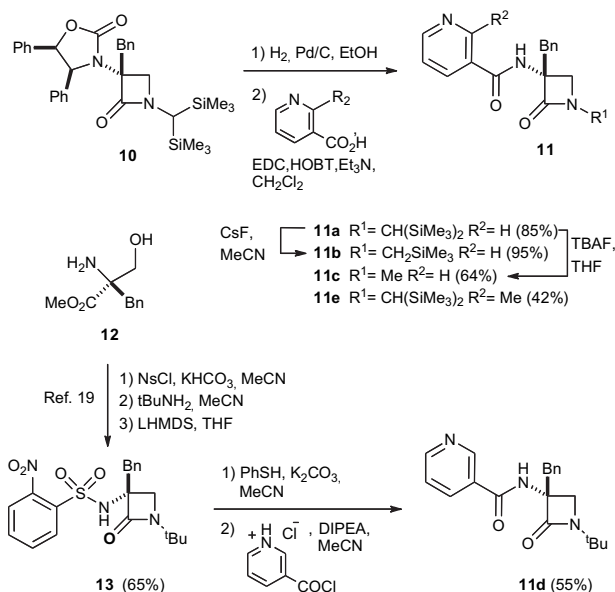


- |  |                     |   |                                  |
|--|---------------------|---|----------------------------------|
| a R <sup>1</sup> = CH(SiMe <sub>3</sub> ) <sub>2</sub> | R <sup>2</sup> = H  | 5 Ar= Ph  | R <sup>3</sup> = Me              |
| b R <sup>1</sup> = CH <sub>2</sub> SiMe <sub>3</sub>   | R <sup>2</sup> = H  | 6 Ar= Ph  | R <sup>3</sup> = Et              |
| c R <sup>1</sup> = Me                                  | R <sup>2</sup> = H  | 7 Ar= Ph  | R <sup>3</sup> = <sup>t</sup> Bu |
| d R <sup>1</sup> = <sup>t</sup> Bu                     | R <sup>2</sup> = H  | 8 Ar= 4-MeOC <sub>6</sub> H <sub>4</sub>              | R <sup>3</sup> = Me              |
| e R <sup>1</sup> = CH(SiMe <sub>3</sub> ) <sub>2</sub> | R <sup>2</sup> = Me | 9 Ar= 4-NO <sub>2</sub> C <sub>6</sub> H <sub>4</sub> | R <sup>3</sup> = Et              |

**Figure 3.**  $\beta$ -Lactam 1,4-dihydronicotinamides prepared and aroyl benzoylformates reduced.

bis[trimethylsilyl]methyl substituent of **4a**. Compound **4e** (R<sup>2</sup>=Me) was chosen as 2-methyl-substituted dihydropyridines are known to reduce carbonyl compounds in very high enantioselectivities.<sup>6d,10d,17</sup> Among the reaction substrates, we selected the aroylformate esters **5–9** containing differently sized R<sup>3</sup> ester groups and aromatic rings with both electron-donating and electron-attracting groups.

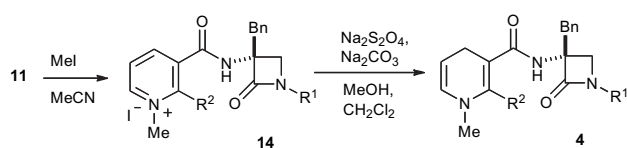
The synthesis of NADH models **4a–e** involved the preparation of their nicotinamide precursors **11a–e** as disclosed in Scheme 1. Accordingly, the *N*-[bis(trimethylsilyl)methyl]- $\beta$ -lactams **11a** and **11e** were first obtained from **10**<sup>18</sup> upon hydrogenolytic *N*-deprotection of the diphenyloxazolidinone moiety, followed by acylation of the intermediate  $\alpha$ -amino- $\beta$ -lactam with nicotinic acid or 2-methylnicotinic acid in the presence of EDC. Then, **11a** was submitted to partial or total chemoselective desilylation<sup>18c</sup> with cesium fluoride or tetra-*n*-butylammonium fluoride to provide, respectively, the mono-silylated derivative **11b** and the *N*-methyl- $\beta$ -lactam **11c** in fair yields. Conversely, the synthesis of the *N*-*tert*-butyl- $\beta$ -lactam **11d** was accomplished following a procedure developed in our laboratory,<sup>19</sup> which used the (*R*)-2-benzyl-serine methyl ester **12** as starting material.<sup>20</sup> After treating this compound with nosyl chloride and KHCO<sub>3</sub> in dry acetonitrile, the resulting *N*-nosylaziridine intermediate was reacted successively with *tert*-butylamine and lithium bis(trimethylsilyl)amide<sup>21</sup> to give the desired *N*-nosyl  $\beta$ -lactam **13** in 65% overall yield. Further deprotection of the nosyl group and coupling of the intermediate  $\alpha$ -amino- $\beta$ -lactam with nicotinyl chloride hydrochloride in the presence of DIPEA afforded the nicotinamide **11d**.



**Scheme 1.** Synthesis of  $\alpha$ -nicotinylamido- $\beta$ -lactams **11**. <sup>a</sup>Key: EDC=1-[3-(dimethylamino)propyl]-3-ethyl carbodiimide hydrochloride; HOBT=1-hydroxybenzotriazole; DIPEA=*N,N*-diisopropylethylamine; TBAF=tetra-*n*-butylammonium fluoride; LHMS=lithium hexamethyldisilazide.

Next, nicotinamides **11** were quantitatively *N*-alkylated with methyl iodide and the resulting pyridinium salts **14a–e** were submitted to regioselective reduction with a mixture of sodium dithionite and sodium carbonate.<sup>22</sup> The desired 1,4-dihydronicotinamides **4** were obtained in good overall yields with the exception of 2-methyl-1,4-dihydronicotinamide **4e**, which afforded complex mixtures under such conditions. Fortunately, a 49% yield of pure **4e** product could be attained when the reduction of **14e** was carried out using sodium bicarbonate as a base (Table 1).<sup>23</sup>

**Table 1**  
Preparation of 1,4-dihydronicotinamide- $\beta$ -lactams **4** from nicotinamides **11**



Entry	R <sup>1</sup>	R <sup>2</sup>	Product	Yield (%)	Product	Yield (%)
1	CH(SiMe <sub>3</sub> ) <sub>2</sub>	H	<b>14a</b>	100	<b>4a</b>	64
2	CH <sub>2</sub> SiMe <sub>3</sub>	H	<b>14b</b>	96	<b>4b</b>	84
3	Me	H	<b>14c</b>	98	<b>4c</b>	82
4	<sup>t</sup> Bu	H	<b>14d</b>	87	<b>4d</b>	74
5	CH(SiMe <sub>3</sub> ) <sub>2</sub>	Me	<b>14e</b>	72	<b>4e<sup>a</sup></b>	47

<sup>a</sup> NaHCO<sub>3</sub> was used as a base instead of Na<sub>2</sub>CO<sub>3</sub>.

## 2.2. Reduction of alkyl aroylformates with $\beta$ -lactam NADH models **4**

Reduction of alkyl aroylformates **5–9** with NADH models **4a–e** was studied at 300 K in the presence of an equivalent of magnesium perchlorate. The reactions were conducted in deuterated acetonitrile and followed by monitoring the NMR spectra of the mixtures. Results summarized in Table 2 showed that a uniform stereo-inducing bias for (*S*) enantiomers prevailed in all instances, irrespective of the nature of the peripheral R<sup>1</sup>, R<sup>2</sup> and R<sup>3</sup> groups. However, the enantiomeric excess of the reactions was sensitive to the size of such groups.

We first checked the stereomodulating effect of the R<sup>1</sup> substituent attached to the  $\beta$ -lactam nitrogen of NADH models **4a–d** on the reduction of methyl benzoylformate **5**. Accordingly, replacement of the bulky bis(trimethylsilyl) methyl group in model **4a** by the less hindered bis(trimethylsilyl)methyl and methyl groups (models **4b** and **4c**, respectively) resulted in an enantiomeric excess decay from 78% to 60% (entries 1–3). Changing to the bulkier model **4d** with a *tert*-butyl group, restored the enantiomeric excess to 78% (entry 4). These data strongly suggested the existence of a direct relationship between the size of R<sup>1</sup> and the enantioselectivity of the reactions. On the other hand, the reduction of methyl benzoylformate **5** with the 2-methyl-NADH  $\beta$ -lactam model **4e** (entry 5) proceeded with poor enantiomeric excess (30%), in contrast to previous reports anticipating very high enantioselectivities for other 2-methyl-substituted NADH models.<sup>17</sup> Therefore, an (unexpected) inverse relationship was

found between the size of the R<sup>2</sup> group and the enantioselectivity of the reaction.

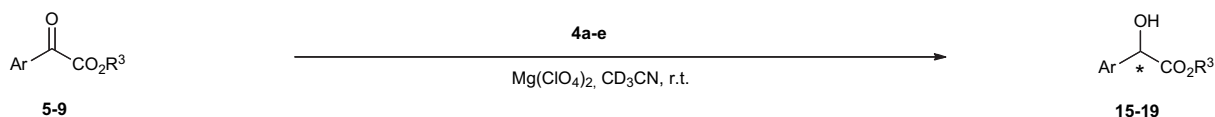
The stereoreductive ability of NADH model **4a** was further tested for different  $\alpha$ -keto esters (**5–9**). Ethyl and *tert*-butyl benzoylformates **6** and **7** were reduced in slightly higher enantiomeric excess (82 and 92%, respectively) than methyl benzoylformate **5** (78%), suggesting that an increase of the R<sup>3</sup> ester group size might also favor higher enantioselectivities. Finally (entries 8 and 9), the stereomodulating effect of electron-donating (OMe, **8**) and electron-withdrawing (NO<sub>2</sub>, **9**) groups placed at the aromatic ring of the aroylformate esters was also tested. As expected from their different chelating ability with Mg<sup>2+</sup> cation, electron-rich substrates favored a slight increase in enantiomeric excess values (compare entries 1 and 8), whereas electron-poor substrates resulted in lower enantiomeric excess (compare entries 6 and 9).

## 2.3. Computational calculations

To investigate the correlation of the stereochemical results collected in Table 2 with our biomimetic reaction model based on chelated ternary complexes NADH/Mg<sup>2+</sup>/ArCOCO<sub>2</sub>R and transition states TS-I (see Fig. 2), a computational study was carried out using the functional B3LYP<sup>24</sup> and the 6-31G\* basis sets as implemented in Gaussian 03.<sup>25</sup>

Reaction free energy differences ( $\Delta\Delta G^\ddagger$ ) expected for enantiomeric excess values below 90% are in the range of 2 kcal/mol. Therefore, it was essential to limit the conformational energy of the calculated reaction intermediates and transition states in order to make a reliable interpretation of the computational data. Accordingly, we designed the simplified  $\beta$ -lactam NADH structures **20–22** (Table 3) with the partially flexible benzyl substituent of compounds **4a–e** (Fig. 3) replaced by the rigid methyl group at the  $\alpha$  position of the  $\beta$ -lactam ring. To gauge the steric effect of the peripheral R<sup>1</sup>, R<sup>2</sup>, and R<sup>3</sup> groups on the enantioselectivity of the alkyl aroylformate reduction reaction, we designed the *N*-methyl- and *N*-*tert*-butyl-substituted models **20** and **21** to represent, respectively, small and large R<sup>1</sup> groups. Similarly, the model **22** incorporating a 2-methyl-dihydropyridine moiety was selected to put into evidence the stereomodulating effect of the R<sup>2</sup> group. Finally, the  $\beta$ -lactam NADH models **20–22** and the substrates **5** (R<sup>3</sup>=Me small group) and **7** (R<sup>3</sup>=*tert*-Bu large group) were combined in four computational reactions (**A–D**, see Table 3) and the corresponding  $\Delta\Delta G^\ddagger$  values were calculated.

**Table 2**  
Reduction of alkyl aroylformates **5–9** with  $\beta$ -lactam NADH models **4a–e**



Entry	NADH model	R <sup>1</sup>	R <sup>2</sup>	Substrate	Ar	R <sup>3</sup>	Product	Reaction time (h) <sup>a</sup>	Yield (%) <sup>b</sup>	ee (%) <sup>c</sup>	Config.
1	<b>4a</b>	CH(SiMe <sub>3</sub> ) <sub>2</sub>	H	<b>5</b>	Ph	Me	<b>15</b>	14	66	78	<i>S</i>
2	<b>4b</b>	CH <sub>2</sub> SiMe <sub>3</sub>	H	<b>5</b>	Ph	Me	<b>15</b>	72	48	65	<i>S</i>
3	<b>4c</b>	Me	H	<b>5</b>	Ph	Me	<b>15</b>	24	60	60	<i>S</i>
4	<b>4d</b>	<sup>t</sup> Bu	H	<b>5</b>	Ph	Me	<b>15</b>	16	70	78	<i>S</i>
5	<b>4e</b>	CH(SiMe <sub>3</sub> ) <sub>2</sub>	Me	<b>5</b>	Ph	Me	<b>15</b>	18	30	30	<i>S</i>
6	<b>4a</b>	CH(SiMe <sub>3</sub> ) <sub>2</sub>	H	<b>6</b>	Ph	Et	<b>16</b>	18	70	92	<i>S</i>
7	<b>4a</b>	CH(SiMe <sub>3</sub> ) <sub>2</sub>	H	<b>7</b>	Ph	<sup>t</sup> Bu	<b>17</b>	22	43	88	<i>S</i>
8	<b>4a</b>	CH(SiMe <sub>3</sub> ) <sub>2</sub>	H	<b>8</b>	4-MeOC <sub>6</sub> H <sub>4</sub>	Me	<b>18</b>	40	35	90	<i>S</i>
9	<b>4a</b>	CH(SiMe <sub>3</sub> ) <sub>2</sub>	H	<b>9</b>	4-NO <sub>2</sub> C <sub>6</sub> H <sub>4</sub>	Et	<b>19</b>	22	63	82	<i>S</i> <sup>d</sup>

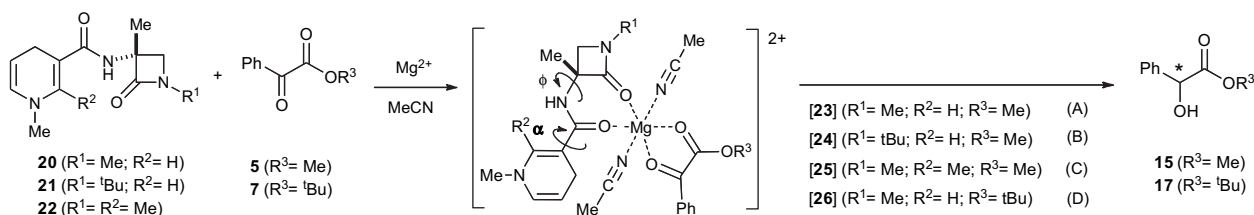
<sup>a</sup> Reactions were quenched when complete consumption of NADH model was observed by <sup>1</sup>H NMR.

<sup>b</sup> Calculated from <sup>1</sup>H NMR spectra on the basis of NAD<sup>+</sup> formation.

<sup>c</sup> Determined by HPLC.

<sup>d</sup> Configuration assigned on the basis of the relative chiral HPLC retention time.

**Table 3**  
Relative energies (in kcal/mol<sup>-1</sup>) and main torsion angles of the [β-lactam NADH (20–22)/Mg<sup>2+</sup>/PhCOCO<sub>2</sub>R<sup>3</sup> (5, 7)] ternary complexes 23–26 and transition structures thereof computed at B3LYP/6-31G<sup>-</sup> level for the reactions (A)–(D)



Entry	Reaction	Ternary complex <sup>a</sup>	ΔG <sup>o</sup> <sub>rel</sub> <sup>b</sup>	TS <sup>1,c</sup>	ΔG <sup>‡d</sup>	ΔΔG <sup>‡</sup> <sub>(R-S)</sub> <sup>e</sup>	α <sup>f</sup>	φ <sup>f</sup>
1	(A)	23S	0.0	23S-syn <sup>+</sup>	22.4	0.0	23.1	62.0
2	(A)	23S	0.0	23S-anti	25.9	—	-87.3	60.2
3	(A)	23R	0.6	23R-syn <sup>+</sup>	25.5	3.1 (3.7)	-20.9	-10.7
4	(A)	23R	0.6	23R-anti	26.6	—	132.0	4.3
5	(B)	24S	1.3	24S-syn <sup>+</sup>	22.7	0	22	63
6	(B)	24S	1.3	24S-anti	22.7	—	-83	60
7	(B)	24R	0.0	24R-anti	27.4	—	130.5	7.5
8	(B)	24R	0.0	24R-syn <sup>+</sup>	27.4	4.7 (4.8)	-18	-5.6
9	(C)	25S-1	0.0	25S-syn1	21.3	—	29.1	61.4
10	(C)	25S-2	2.2	25S-syn2	24.9	—	-13.8	67.7
11	(C)	25S-2	2.2	25S-anti2 <sup>*</sup>	20.1	0.0	96.3	60.6
12	(C)	25R-1	4.0	25R-syn1 <sup>+</sup>	22.0	1.9 (2.4)	121.9	11.1
13	(C)	25R-1	4.0	25R-anti1	25.9	—	28.0	-6.8
14	(C)	25R-2	1.7	25S-syn2	25.8	—	-28.0	-12.8
15	(D)	26S	0.8	26S-syn <sup>+</sup>	25.8	0.0	22.6	60.2
16	(D)	26S	0.8	26S-anti	29.8	—	-83.5	60.2
17	(D)	26R	0.0	26R-anti <sup>+</sup>	29.3	3.5 (4.6)	131.9	4.4
18	(D)	26R	0.0	26R-syn	29.8	—	-21.2	-10.6

<sup>a</sup> Descriptors *R* and *S* denote the configuration of the final mandelate product; '1' and '2' descriptors denote, respectively, positive and negative α dihedral angles (see text).

<sup>b</sup> Relative ΔG<sup>o</sup> formation energies calculated from the most stable ternary complexes 23–36 in each reaction (A)–(D).

<sup>c</sup> Transition states with asterisk identify the lowest energy pathways to the *R* and *S* enantiomer products.

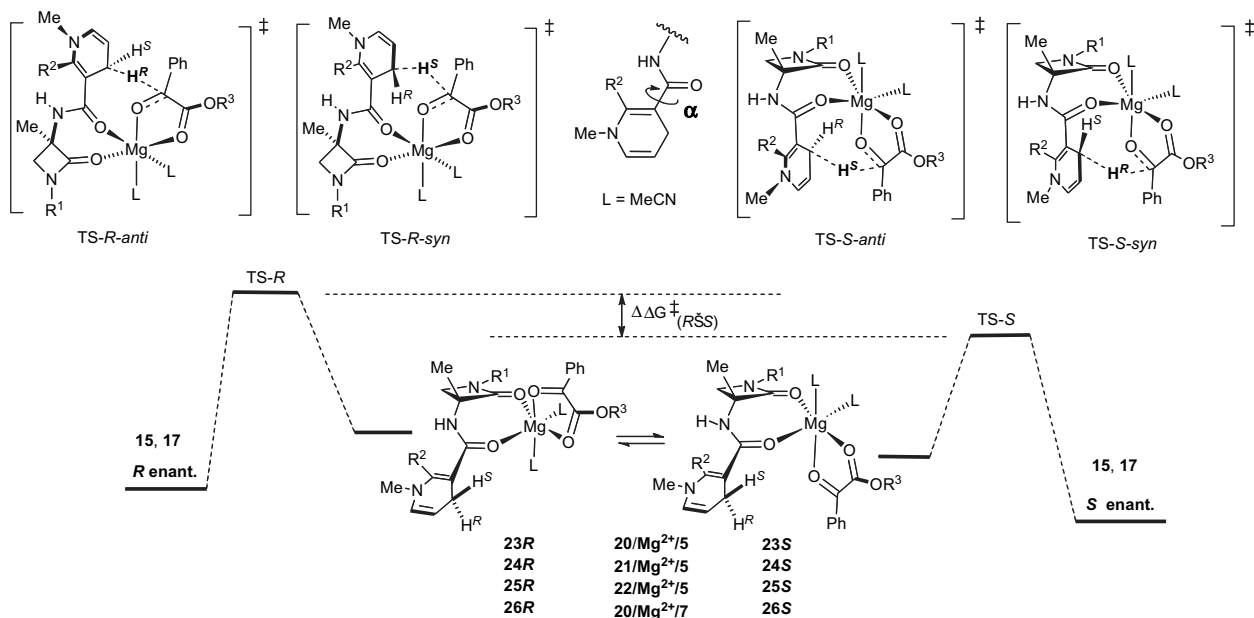
<sup>d</sup> Relative ΔG<sup>‡</sup> activation energies calculated from the most stable ternary structures 23–36 in each reaction (A)–(D).

<sup>e</sup> Values in parentheses correspond to activation energy differences after single-point refinement at B3LYP/6-311++G<sup>++</sup> level including the IEF-PCM solvation model (MeCN, ε=36.64).

<sup>f</sup> Dihedral angles of the transition states as defined in Figure 1.

As outlined in Scheme 2, the reaction mechanism proposed<sup>14</sup> involved the initial formation of the ternary complexes NADH/Mg<sup>2+</sup>/PhCOCO<sub>2</sub>R<sup>3</sup> 23–26, which were formally built up from [Mg(NCMe)<sub>6</sub>]<sup>2+</sup> by displacement of four acetonitrile ligands with

the β-lactam NADH models 20–22 and alkyl benzoylformates 5 and 7. In all instances, the bonding patterns were created assuming an octahedral coordination geometry for the Mg<sup>2+</sup> cation.<sup>26</sup> The ternary complexes 23S–26S and 23R–26R, leading, respectively to the



**Scheme 2.** Structures of productive ternary complexes (NADH/Mg<sup>2+</sup>/PhCO<sub>2</sub>R<sup>3</sup>) 23–26 and transition states leading to *R* and *S* mandelate enantiomers. Rotation of the dihydronicotinamide moiety around the α torsion angle in each complex prompts the transfer of H<sup>S</sup> or H<sup>R</sup> hydride atoms through *syn*- or *anti*-transition states. Energy levels are not depicted linearly.

major *S* and minor *R* enantiomeric products, were also assumed to participate in a ligand exchange equilibrium. After B3LYP/6-31G\* calculation (Table 3, column 4), only small stability-differences were recorded between the conformers of the ternary complexes **23**, **24**, and **26** (0.6–1.3 kcal/mol), whereas the  $\Delta G_{\text{rel}}^{\circ}$  formation energies of conformers **25** differed from each other in up to 4.0 kcal/mol. In addition, the number of computationally characterizable complexes **25** for reaction **C** increased from two to four, as a result of the hindered rotation around the  $\alpha$  torsion angle caused by the methyl group ( $R^2$ ) attached to the dihydronicotinamide ring. Next, we studied the reaction step determining the rate and enantioselectivity of the reactions **A–D**, which involved the concerted intramolecular hydrogen atom transfer from the dihydronicotinamide  $C_4$  position to the aroylformate ketone. Depending on the diastereotopic hydrogen atom ( $H^R$  or  $H^S$ ) transferred to the carbonyl carbon, the transition states arising from each ternary complex could adopt two topologies (see Scheme 2) to form the mandelate products. These conformations were defined as *syn/anti* on the basis of the  $\alpha$  torsion angle describing the relative disposition of the dihydronicotinamide ring with respect to the carbonyl group (see also Fig. 1).

An inspection of the relative free energies and the key dihedral angles ( $\alpha, \varphi$ ) of the transition states TS-**23–26** summarized in Table 3 clearly suggested the existence of a relationship between the steric size of each peripheral  $R^1$ ,  $R^2$ ,  $R^3$  groups, and the  $\Delta\Delta G_{(R-S)}^{\ddagger}$  governing the enantiomeric excesses of reactions **A–D**. For instance, the activation energy differences ( $\Delta\Delta G^{\ddagger}$ ) computed for the reduction of methyl  $\alpha$ -keto ester **5** with the *N*-methyl- $\beta$ -lactam **20** (reaction **A**) and the *N*-*tert*-butyl- $\beta$ -lactam **21** (reaction **B**) were 3.1 and 4.7 kcal/mol, respectively. Although these absolute values and their relative increment were clearly overestimated with respect to the expected enantiomeric excesses, they reflected the enantiomeric excess increase bias observed experimentally for the reduction of methyl benzoylformate **5** with **4c** and **4d** (entries 3 and 4 in Table 2). Hence, the enantiomeric excess increase recorded experimentally by increasing the size of the  $R^1$  group was fully consistent with our model.

The significant enantiomeric excess drop of 48% observed for the reduction of methyl benzoylformate with compound **4a** and the 2-methyl-dihydronicotinamide model **4e** (compare entries 1 and 5 in Table 2) could also be conveniently interpreted on the basis of our mechanistic model. Indeed,  $\Delta\Delta G_{(R-S)}^{\ddagger}$  values decreased from 3.1 for reaction **A** to 1.9 kcal/mol for reaction **C**. A careful inspection of the geometry of structures TS-**25S-anti2** and TS-**25R-syn1** revealed that the methyl group in the NADH ring caused some steric distortion around the  $\alpha$  dihedral angle, diffculting a proper O=C=C  $\pi$ - $\pi$  conjugation. This effect could be at the origin of the detrimental effect on the enantiomeric excess caused by an increase of the size of the  $R^2$  group (see Supplementary data for details).

The computational reduction of *tert*-butyl benzoylformate **7** with the  $\beta$ -lactam model **20** yielded a  $\Delta\Delta G_{(R-S)}^{\ddagger}$  value of 3.5 kcal/mol for reaction **D** (Table 3), which was slightly higher than the 3.1 kcal/mol activation energy difference for the reduction of methyl benzoylformate **5** with the same NADH model (reaction **A**). Again, the calculated data reflected the experimental enantiomeric excess increase of 10% observed by comparing the examples of entries 1 and 7 in Table 2 and explained satisfactorily the beneficial effect of a larger benzoylformate  $R^3$  ester group on the reaction enantiomeric excess.

Finally, to estimate the solvent effect of acetonitrile on the reactions studied, single-point calculations with the self-consistent reaction field (SCRF) based on the IEF-PCM<sup>27</sup> solvation model (MeCN,  $\epsilon=36.64$ ) were performed at B3LYP/6-311++G\*\* level. This analysis resulted in an homogeneously biased increase of  $\Delta\Delta G^{\ddagger}$  values in 0.1–1.1 kcal/mol for the previously optimized productive

transition states TS-**23–26** (see Table 3) and confirmed every peripheral stereomodulating effect calculated for  $R^1$ ,  $R^2$ , and  $R^3$  groups at B3LYP/6-31G\* level.

### 3. Conclusions

A mechanistic model accounting for the stereoinducing behavior observed during the  $Mg^{2+}$ -promoted nonenzymatic NADH reduction of alkyl aroylformates has been proposed on the basis of NADH/ $Mg^{2+}$ /ArCOCO<sub>2</sub> $R^3$  ternary complexes chelated around an octahedral magnesium cation. Using rigidified  $\beta$ -lactam dihydronicotinamides to minimize conformational energy, we have predicted not only the stereoinducing sense of the reaction, but also the stereomodulating trend exerted by remote groups placed in the peripheral positions of the complex. Despite its general bias to overweight the activation energies under B3LYP/6-31G\* computation level, our model represents a valuable conceptual tool to understand important mechanistic aspects of the stereoselective reduction of alkyl aroylformates with non-enzymatic NADH models.

## 4. Experimental section

### 4.1. General experimental

All reactions were carried out under nitrogen or argon atmosphere in oven or flame-dried glassware with magnetic stirring. Solvents were distilled prior to use. Tetrahydrofuran (THF) was distilled from sodium metal/benzophenone ketyl. Dichloromethane ( $CH_2Cl_2$ ) was distilled from calcium hydride. Dichloromethane, methanol, water, and deuterated acetonitrile ( $CD_3CN$ ) used for preparation of NADH models and for biomimetic reductions were deoxygenated by nitrogen bubbling for 2–3 h or by freeze–pump–thaw techniques. Magnesium perchlorate was dried by heating under vacuum for 24 h, and then deoxygenated using standard Schlenk techniques. Purification of reaction products was carried out by flash chromatography using silica gel 60 (230–400 mesh, from Merck 60F PF254). Analytical thin layer chromatography was performed on 0.25 mm silica gel 60-F plates. Visualization was accomplished with UV light and phosphomolybdic acid/ammonium cerium (IV) nitratesulfuric acid/water reagent, followed by heating. Melting points were measured with a Büchi SMP-20 melting point apparatus and are uncorrected. Infrared spectra were recorded on a Shimadzu IR-435 spectrophotometer. NMR spectra were recorded on Bruker Avance500 spectrometers at frequencies of 500 MHz for <sup>1</sup>H NMR and 125 MHz for <sup>13</sup>C NMR, at room temperature unless otherwise stated. Chemical shifts are reported in parts per million (ppm) relative to the central line of  $CD_2Cl_2$  (5.33 ppm),  $CDCl_3$  (7.28 ppm), and  $CD_3CN$  (1.94 ppm) for <sup>1</sup>H NMR, and to the central line of  $CD_2Cl_2$  (54.0 ppm),  $CDCl_3$  (77.0 ppm) and  $CD_3CN$  (1.39 ppm) for <sup>13</sup>C NMR. Combustion analyses were performed on a Leco CHNS-932 elemental analyzer. Enantiomeric excesses were determined by analytical high performance liquid chromatography (HPLC) on a Hewlett Packard 1050 chromatograph equipped with a diode array UV detector and on a Waters 600 chromatograph equipped with a Waters 2487 Dual  $\lambda$  absorbance detector using the chiral columns Chiralcel OD, Chiralcel OB-H, Chiralcel OJ, and Chiralpak AD with flow rates of 0.7 mL/min and 0.5 mL/min (mobile phase hexane/isopropanol). Optical rotations were measured at 25±0.2 °C in methylene chloride unless otherwise stated. Mass spectra were obtained on a Finnigan GCQ mass spectrometer (70 eV) using GC–MS coupling (column: fused silica gel, 15 m, 0.25 mm, 0.25 nm phase SPB-5). Preparation and physical data of compounds **4a**, **c**, **10**, **11a**, **11**, **12**, **14a**, and **c** have been reported previously.<sup>14,19</sup>

#### 4.2. (3R)-3-Benzyl-1-(1-tert-butyl)-3-(2-nitrobenzenesulfonylamino)-azetid-2-one (13)

To a stirred solution of  $\alpha$ -benzyl-serine methyl ester (1 mmol, 0.209 g) in dry acetonitrile (20 mL) *o*-nosyl chloride (2.2 mmol, 0.45 g), and  $\text{KHCO}_3$  (5 mmol) were added. The mixture was stirred at reflux for 8–24 h. After checking an aliquot by  $^1\text{H}$  NMR, freshly distilled *tert*-butylamine (0.073 g) dissolved in a minimum volume of dry  $\text{CH}_2\text{Cl}_2$  was added at rt. The mixture was stirred at rt overnight (followed by  $^1\text{H}$  NMR), and then was filtered over a Celite pad and the intermediate  $\beta$ -amino ester was purified by flash-column chromatography (silica gel; eluent: hexane/EtOAc). This product was dissolved in dry THF (20 mL) and the temperature of the mixture was cooled down to 0–5 °C. Then, a solution of LiHMDS (1 M) in THF (2.5 mmol) was slowly added while a deep purple color developed. The mixture was stirred for 1 h at this temperature and then it was quenched with  $\text{NaHCO}_3$  (20 mL). The aqueous phase was extracted with  $\text{CH}_2\text{Cl}_2$  (3  $\times$  20 mL), the collected organic fractions were dried ( $\text{MgSO}_4$ ), filtered, and the solvent was removed in vacuo. The product was purified by column chromatography (silica gel; eluent: hexanes/EtOAc). Yield: 65%, 0.271 g; oil;  $[\alpha]_D^{25} -47.5$  ( $c=1.0$ ,  $\text{CH}_2\text{Cl}_2$ ); IR ( $\text{cm}^{-1}$ , KBr): 1744; 1646 ( $\text{C}=\text{O}$ ). HPLC-MS, MeOH/HCOOH  $m/z$  (ion source type: ESI, positive polarity): MS+1: 418.1, MS2 (418.1): 390.1, 334.0, 147.0, MS3 (390.0): 334.0, 317.0, 147.0, 130.0.  $^1\text{H}$  NMR ( $\delta$ , ppm,  $\text{CDCl}_3$ ): 8.20 (dd, 1H,  $J_1=1.4$  Hz,  $J_2=7.8$  Hz), 7.89 (dd, 1H,  $J_1=1.4$  Hz,  $J_2=7.8$  Hz), 7.74 (m, 2H), 7.29–7.26 (m, 5H), 5.91 (br s, 1H), 3.65 (d, 1H,  $J=5.5$  Hz), 3.32 (d, 1H,  $J=5.5$  Hz), 3.09 (br s, 2H), 1.10 (s, 3H).  $^{13}\text{C}$  NMR ( $\delta$ , ppm,  $\text{CDCl}_3$ ): 164.4, 147.7, 135.8, 133.7, 133.1, 131.3, 130.3, 128.8, 127.8, 125.6, 68.0, 53.2, 49.2, 47.6, 40.5, 29.9, 28.8, 27.6. Anal. Calcd for  $\text{C}_{20}\text{H}_{23}\text{N}_3\text{O}_5\text{S}_2$  (417.48): C, 57.54; H, 5.55; N, 10.07. Found: C, 57.25; H, 5.73; N, 9.70.

#### 4.3. Preparation of $\alpha$ -(2-nicotinamido)- $\beta$ -lactams 11

4.3.1. (3R)-3-Benzyl-1-[(trimethylsilyl)methyl]-3-nicotinamido-azetid-2-one (11b). A solution of the  $\beta$ -lactam-nicotinamide **11a** (0.25 mmol, 0.110 g) in  $\text{CH}_3\text{CN}$  (5 mL) under nitrogen atmosphere was heated at 70 °C, and then cesium fluoride (3 equiv, 0.75 mmol, 0.114 g) was added. The reaction mixture was heated at 70 °C for 1 h (consumption of starting material was checked by TLC, eluent EtOAc). The solvent was evaporated under reduced pressure and the crude reaction mixture was dissolved in dichloromethane, and washed with water (2  $\times$  5 mL). The organic phase was dried over  $\text{MgSO}_4$  and the solvents were evaporated to afford the desired product, which was used without further purification. Yield: 0.088 g (95%); oil;  $[\alpha]_D^{25} -11.0$  ( $c=1.0$ ,  $\text{CH}_2\text{Cl}_2$ ); IR ( $\text{cm}^{-1}$ , KBr): 3448; 2934; 1732 ( $\text{C}=\text{O}$ ); 1662 ( $\text{C}=\text{O}$ ); 854 ( $\text{C}-\text{Si}$ ). HPLC-MS, MeOH/HCOOH  $m/z$  (ion source type: ESI, positive polarity): MS+1: 368.1, MS2 (468.2): 253.0 MS3 (253.0): 225.0, 191.9, 174.9, 134.0, 106.1.  $^1\text{H}$  NMR ( $\delta$ , ppm,  $\text{CDCl}_3$ ): 8.97 (br s, 1H), 8.71 (br s, 1H), 8.08 (d, 1H,  $J=8.0$  Hz), 7.33–7.25 (m, 5H), 3.63 (d, 1H,  $J=6.0$  Hz), 3.46 (d, 1H,  $J=6.0$  Hz), 3.32 (d, 1H,  $J=13.7$  Hz), 3.27 (d, 1H,  $J=13.7$  Hz), 2.69 (d, 1H,  $J=15.4$  Hz), 2.50 (d, 1H,  $J=15.4$  Hz),  $-0.04$  (s, 9H).  $^{13}\text{C}$  NMR ( $\delta$ , ppm,  $\text{CDCl}_3$ ): 167.3, 165.7, 152.7, 148.76, 135.2, 130.5, 128.9, 127.5, 123.6, 68.8, 53.7, 39.0, 34.0, 29.9,  $-1.8$ . Anal. Calcd for  $\text{C}_{20}\text{H}_{25}\text{N}_3\text{O}_2\text{Si}$  (367.52): C, 65.36; H, 6.86; N, 11.43. Found: C, 65.78; H, 6.68; N, 11.86.

4.3.2. (3R)-3-Benzyl-1-(tert-butyl)-3-nicotinamido-azetid-2-one (11d). To a solution of the nicotinoyl chloride hydrochloride **27** (2 mmol, 356 g) in 25 mL of dry  $\text{CH}_3\text{CN}$  cooled to  $-5$  °C under nitrogen atmosphere, *N,N*-diisopropylethylamine (DIPEA) (6.4 mmol, 1.1 mL), and a solution of the corresponding  $\alpha$ -amino- $\beta$ -lactam (0.8 mmol, 0.186 g) in 10 mL  $\text{CH}_3\text{CN}$  were added. The reaction mixture was stirred for 1 h at 0 °C, then at rt (5–18 h, monitored by  $^1\text{H}$  NMR). After that time,  $\text{CH}_2\text{Cl}_2$  (20 mL) was added and the

solution was washed with NaOH 0.1 M (20 mL),  $\text{NH}_4\text{Cl}$  (20 mL), and  $\text{H}_2\text{O}$  (20 mL). The organic phase was decanted and dried over  $\text{MgSO}_4$ . The solvents were evaporated under reduced pressure and the crude was purified by flash chromatography, eluent: EtOAc. Yield: 0.149 g (55%); oil;  $[\alpha]_D^{25} -11$  ( $c=1.0$ ,  $\text{CH}_2\text{Cl}_2$ ); IR ( $\text{cm}^{-1}$ , KBr): 1743.4 ( $\text{C}=\text{O}$ ); 1661.2 ( $\text{C}=\text{O}$ ); 1248.0 (*tert*-Bu). HPLC-MS, MeCN/HCOOH  $m/z$  (ion source type: ESI, positive polarity): MS+1: 338.2, MS2 (338.2): 253.0, MS3 (188.0): 174.9, 134.0, 106.1.  $^1\text{H}$  NMR ( $\delta$ , ppm,  $\text{CDCl}_3$ ): 9.00 (d, 1H,  $J=1.7$  Hz), 8.75 (dd, 1H,  $J_1=1.4$  Hz,  $J_2=4.7$  Hz), 8.13–8.10 (m, 1H), 8.38 (br s, 1H), 7.40–7.32 (m, 6H), 7.02 (br s, 1H), 3.60 (d, 1H,  $J=5.9$  Hz), 3.43 (d, 1H,  $J=5.9$  Hz), 3.37 (d, 1H,  $J=13.5$  Hz), 3.24 (d, 1H,  $J=13.5$  Hz), 1.12 (s, 9H).  $^{13}\text{C}$  NMR ( $\delta$ , ppm,  $\text{CDCl}_3$ ): 165.9, 165.7, 152.6, 148.8, 135.4, 135.0, 130.6, 127.5, 129.6, 128.7, 127.45, 123.52, 66.03, 53.16, 47.74, 39.00, 27.44. Anal. Calcd for  $\text{C}_{20}\text{H}_{23}\text{N}_3\text{O}_2$  (337.42): C, 71.19; H, 6.87; N, 12.45. Found: C, 71.16; H, 6.91; N, 12.85.

#### 4.4. (3R)-3-Benzyl-1-[bis(trimethylsilyl)methyl]-3-(2-methylnicotinamido)-azetid-2-one (11e)

A solution of the corresponding amine (1.62 mmol, 0.543 g) in dry  $\text{CH}_2\text{Cl}_2$  (20 mL) under nitrogen atmosphere was cooled to 0 °C. Then, 2-methylnicotinic acid (1.5 equiv, 2.43 mmol, 0.335 g),  $\text{NET}_3$  (1.5 equiv, 2.43 mmol, 0.54 mL), HOBT (1.5 equiv, 2.43 mmol, 1.20 g), and EDC  $\cdot$  HCl (1.5 equiv, 2.43 mmol, 0.47 g) were added. The stirring was continued for an hour at 0 °C, and for 24 h at rt. After that time,  $\text{CH}_2\text{Cl}_2$  (10 mL) was added and the solution was washed with 1 M aqueous  $\text{KHSO}_4$  (20 mL) and  $\text{H}_2\text{O}$  (20 mL). The organic phase was decanted and dried over  $\text{MgSO}_4$ . The solvents were evaporated under reduced pressure and the crude was purified by flash-column chromatography (eluent EtOAc). Yield: 0.53 g (73%); oil;  $[\alpha]_D^{25} +4.8$  ( $c=1.0$ ,  $\text{CH}_2\text{Cl}_2$ ); IR ( $\text{cm}^{-1}$ , KBr): 1733.5 ( $\text{C}=\text{O}$ ); 1664.6 ( $\text{C}=\text{O}$ ); 848.0 ( $\text{C}-\text{Si}$ ). HPLC-MS, MeOH/HCOOH  $m/z$  (ion source type: ESI, positive polarity): MS+1: 454.2, MS2 (454.2): 267.0, 188.0, MS3 (267.0): 238.9, 221.0, 205.9, 188.9, 147.9, 120.0.  $^1\text{H}$  NMR ( $\delta$ , ppm,  $\text{CDCl}_3$ ): 8.56 (d, 1H,  $J=4.2$  Hz), 7.54 (d, 1H,  $J=7.4$  Hz), 7.32–7.25 (m, 5H), 7.16 (m, 1H), 7.06 (br s, 1H), 3.76 (d, 1H,  $J=6.3$  Hz), 3.63 (d, 1H,  $J=6.3$  Hz), 3.37 (s, 2H), 2.65 (s, 3H), 2.61 (s, 1H).  $^{13}\text{C}$  NMR ( $\delta$ , ppm,  $\text{CDCl}_3$ ): 170.5, 168.4, 167.0, 156.6, 150.2, 135.5, 131.3, 130.7, 129.0, 127.6, 127.0, 125.0, 121.2, 119.2, 110.2, 68.7, 54.8, 39.0, 38.2, 22.8,  $-0.05$ ,  $-0.14$ . Anal. Calcd for  $\text{C}_{24}\text{H}_{35}\text{N}_3\text{O}_2\text{Si}_2$  (453.72): C, 63.53; H, 7.78; N, 9.26. Found: C, 63.56; H, 7.18; N, 9.10.

#### 4.5. General procedure for the preparation of pyridinium salts 14

To a solution of the corresponding nicotinamide (1.00 mmol) in  $\text{CH}_3\text{CN}$  (10 mL) under  $\text{N}_2$  atmosphere, methyl iodide (6 mL) was added. The reaction mixture was stirred at 50 °C for 2–24 h. After that time, the solvents were evaporated and the residue was dried under vacuum to afford the pyridinium iodide as a hygroscopic solid, which was used without further purification.

4.5.1. *N*-[(3R)-3-Benzyl-1-[(trimethylsilyl)methyl]-2-oxoazetid-3-yl-1-methylpyridinium]-3-carboxamide iodide (14b). The general procedure was followed (reaction time: 4 h) from **11b** (0.234 mmol, 0.086 g). Yield: 0.111 g (96%); yellow solid; mp: 159–160 °C;  $[\alpha]_D^{25} +3.75$  ( $c=1.0$ ,  $\text{CH}_2\text{Cl}_2$ ); IR ( $\text{cm}^{-1}$ , KBr): 3472; 2958; 1746 ( $\text{C}=\text{O}$ ); 1681 ( $\text{C}=\text{O}$ ); 854 ( $\text{C}-\text{Si}$ ). HPLC-MS, MeOH/HCOOH  $m/z$  (ion source type: ESI, negative polarity): MS-1: 508.2, MS2 (508.2): 426.6, 366.1, 277.0, 126.9.  $^1\text{H}$  NMR ( $\delta$ , ppm,  $\text{CDCl}_3$ ): 9.91 (s, 1H); 9.00 (d, 1H,  $J=6.1$  Hz); 8.92 (d, 1H,  $J=8.1$  Hz); 8.77 (s, 1H); 8.75 (br s, 1H); 8.08 (m, 1H); 7.35–7.30 (m, 5H); 4.59 (s, 3H); 3.68 (d, 1H,  $J=5.4$  Hz); 3.50 (d, 1H,  $J=13.8$  Hz); 3.46 (d, 1H,  $J=13.8$  Hz); 3.26 (d, 1H,  $J=5.4$  Hz); 2.54 (d, 1H,  $J=15.4$  Hz); 2.46 (d, 1H,  $J=15.4$  Hz);  $-0.08$  (s, 9H).  $^{13}\text{C}$  NMR ( $\delta$ , ppm,  $\text{CDCl}_3$ ): 167.6, 161.5, 147.2, 145.3, 145.0, 134.4, 133.4,

130.8, 128.8, 127.5, 69.8, 51.5, 49.9, 38.8, 33.7, –1.9. Anal. Calcd for  $C_{21}H_{28}IN_3O_2Si$  (509.46): C, 49.51; H, 5.54; N, 8.25. Found: C, 49.91; H, 5.50; N, 8.47.

4.5.2. *N*-[(3*R*)-3-Benzyl-1-(*tert*-butyl)-2-oxoazetid-3-yl-1-methylpyridinium]-3-carboxamide iodide (**14d**). The general procedure was followed (reaction time: 2 h) from **11d** (0.44 mmol, 0.149 g). Yield: 0.184 g (87%); oil;  $[\alpha]_D^{25} +8.4$  ( $c=1.0$ ,  $CH_2Cl_2$ ); IR ( $cm^{-1}$ , KBr): 1726.0 (C=O); 1674.2 (C=O). HPLC-MS, MeOH/HCOOH *m/z* (ion source type: ESI, negative polarity): MS-1: 478.1, MS2 (478.1): 380.7, 352.3, 316.8, 276.8, 232.1, 126.8.  $^1H$  NMR ( $\delta$ , ppm,  $CDCl_3$ ): 9.92 (s, 1H); 9.05 (d, 1H,  $J=6.1$  Hz); 8.964 (d, 1H,  $J=8.1$  Hz); 8.70 (s, 1H); 8.13 (dd, 1H,  $J_1=6.2$  Hz,  $J_2=8.0$  Hz); 7.35–7.30 (m, 5H); 4.61 (s, 3H); 3.60 (d, 1H,  $J=5.2$  Hz); 3.47 (d, 1H,  $J=13.5$  Hz); 3.44 (d, 1H,  $J=13.5$  Hz); 3.19 (d, 1H,  $J=5.3$  Hz); 0.99 (s, 9H).  $^{13}C$  NMR ( $\delta$ , ppm,  $CDCl_3$ ): 165.7, 161.4, 147.3, 145.3, 145.0, 134.1, 133.2, 130.9, 128.4, 128.2, 127.4, 66.9, 52.8, 49.7, 45.7, 38.9, 27.2. Anal. Calcd for  $C_{21}H_{26}IN_3O_2$  (479.35): C, 52.62; H, 5.47; N, 8.77. Found: C, 52.82; H, 5.50; N, 8.21.

4.5.3. *N*-[(3*R*)-3-Benzyl-1-(bis(trimethylsilyl)methyl)-2-oxoazetid-3-yl-1,2-dimethylpyridinium]-3-carboxamide iodide (**14e**). The general procedure was followed (reaction time: 24 h) from **11e** (0.5 mmol, 0.2272 g). Yield: 0.282 g (95%); oil; IR ( $cm^{-1}$ , KBr): 1737.0 (C=O); 1674.4 (C=O); 841.7 (C-Si). HPLC-MS, MeOH/HCOOH *m/z* (ion source type: ESI, positive polarity):  $M^+-I$  (iodine loss): 468.2, MS2 (468.2): 281.0, 263.2, 237.0, MS3 (237.0): 220.9, 221.0, 205.9, 188.9, 147.9, 120.0.  $^1H$  NMR ( $\delta$ , ppm,  $CDCl_3$ ): 8.63 (d, 1H,  $J=6.1$  Hz); 8.38 (br s, 1H); 8.14 (d, 1H,  $J=8.5$  Hz); 7.80 (m, 1H); 7.48 (d, 1H,  $J=8.2$  Hz); 7.35–7.28 (m, 3H); 4.26 (s, 3H); 3.92 (d, 1H,  $J=5.7$  Hz); 3.53 (d, 1H,  $J=5.7$  Hz); 3.50 (d, 1H,  $J=14.4$  Hz); 3.42 (d, 1H,  $J=14.4$  Hz); 2.76 (s, 3H); 2.71 (s, 1H); 0.17 (s, 9H); 0.11 (s, 9H).  $^{13}C$  NMR ( $\delta$ , ppm,  $CDCl_3$ ): 166.5, 164.5, 154.7, 147.0, 143.7, 138.2, 135.3, 130.8, 128.9, 127.5, 125.9, 69.4, 54.0, 47.8, 39.2, 37.9, 19.7, 0.2, 0.1.

#### 4.6. General procedure for the preparation of 1,4-dihydropyridines 4

To a solution of the corresponding pyridinium salt (0.5 mmol) in 12 mL of deoxygenated  $CH_2Cl_2/MeOH$  (3/1) a deoxygenated solution of  $Na_2S_2O_4$  (10.0 mmol) in 0.5 M aqueous  $Na_2CO_3$  (12.5 mL) was added and the mixture was vigorously stirred under nitrogen in the dark for 16 h (soon the color of the solution turned from orange to yellow). The organic layer was separated, the aqueous phase was extracted with  $CH_2Cl_2$  (deoxygenated; 10 mL $\times$ 2), and the combined organic phase was dried ( $MgSO_4$ ) and concentrated in vacuo to give the crude corresponding dihydropyridine, which was used in the following reaction without further purification. These compounds can be kept for 24–48 h at  $-30^\circ C$  without oxidation or decomposition.

4.6.1. (3*R*)-3-Benzyl-1-[(trimethylsilyl)methyl]-3-(*N*-methyl-dihydro-nicotinamido)-azetid-2-one (**4b**). The general procedure was followed from **14b** (0.185 mmol, 0.094 g). Yield: 0.059 g (84%); orange solid;  $^1H$  NMR ( $\delta$ , ppm,  $CD_2Cl_2$ ): 7.32–7.25 (m, 5H); 6.88 (d, 1H,  $J=1.4$  Hz); 5.69 (dd, 1H,  $J_1=8.0$  Hz,  $J_2=1.6$  Hz); 5.47 (br s, 1H); 4.68 (m, 1H); 3.56 (d, 1H,  $J=5.4$  Hz); 3.34 (d, 1H,  $J=5.4$  Hz); 3.19 (d, 1H,  $J=13.7$  Hz); 3.15 (d, 1H,  $J=13.7$  Hz); 3.02–2.95 (dm, 2H); 2.91 (s, 3H); 2.68 (d, 1H,  $J=15.4$  Hz); 2.54 (d, 1H,  $J=15.4$  Hz); 0.01 (s, 9H).  $^{13}C$  NMR ( $\delta$ , ppm,  $CD_2Cl_2$ ): 168.7, 167.7, 140.1, 136.3, 130.7, 130.4, 129.0, 127.6, 102.8, 99.0, 68.4, 41.2, 39.9, 33.7, 30.2, 22.6, –1.8.

4.6.2. (3*R*)-3-Benzyl-1-(*tert*-butyl)-3-(*N*-methyl-dihydro-nicotinamido)-azetid-2-one (**4d**). The general procedure was followed from **14d** (0.37 mmol, 0.180 g). Yield: 0.096 g (74%); oil;  $^1H$  NMR ( $\delta$ , ppm,  $CD_2Cl_2$ ): 7.31–7.27 (m, 5H); 7.22 (br s, 1H); 6.89 (d, 1H,

$J=1.3$  Hz); 5.69 (dd, 1H,  $J_1=8.0$  Hz,  $J_2=1.6$  Hz); 5.47 (br s, 1H); 4.69 (m, 1H); 3.50 (d, 1H,  $J=5.4$  Hz); 3.25 (d, 1H,  $J=5.4$  Hz); 3.16 (d, 1H,  $J=13.5$  Hz); 3.10 (d, 1H,  $J=13.5$  Hz); 3.06–2.95 (m, 2H); 2.91 (s, 3H); 1.09 (s, 9H).  $^{13}C$  NMR ( $\delta$ , ppm,  $CD_2Cl_2$ ): 168.2, 167.0, 140.3, 135.8, 130.8, 130.1, 128.7, 127.4, 102.9, 98.6, 65.7, 53.1, 47.9, 41.1, 39.3, 27.6, 22.5.

4.6.3. (3*R*)-3-Benzyl-1-[bis(trimethylsilyl)methyl]-3-[*N*,2-dimethyl-dihydro-nicotinamido]-azetid-2-one (**4e**). The general procedure was followed from **14e** (using  $NaHCO_3$  instead of  $Na_2CO_3$ ) (0.14 mmol, 0.083 g). Yield: 0.027 g (49%); yellow oil;  $^1H$  NMR ( $\delta$ , ppm,  $CD_2Cl_2$ ): 7.27 (m, 5H); 5.80 (br s, 1H); 5.70 (d, 1H,  $J=7.9$  Hz); 4.56 (m, 1H); 3.58 (d, 1H,  $J=5.9$  Hz); 3.47 (d, 1H,  $J=5.9$  Hz); 3.28 (d, 1H,  $J=13.7$  Hz); 3.19 (d, 1H,  $J=13.7$  Hz); 2.96–2.92 (m, 5H); 2.57 (s, 1H); 0.05 (s, 9H); 0.02 (s, 9H).  $^{13}C$  NMR ( $\delta$ , ppm,  $CD_2Cl_2$ ): 169.4, 167.6, 140.1, 136.3, 130.3, 129.06, 127.86, 102.7, 98.8, 68.5, 41.1, 40.0, 28.5, 22.5.

#### 4.7. General procedure for the biomimetic reduction of alkyl aroylformates with NADH peptidomimetics 4

In a typical run, a solution of the NADH model **4** (0.103 mmol, 1.1 equiv),  $Mg(ClO_4)_2$  (0.103 mmol, 1.1 equiv, 23.0 mg), and carbonyl compound (0.093 mmol) in 0.7 mL of deoxygenated  $CD_3CN$  was prepared in a dried NMR tube in the dark and the reaction was followed by  $^1H$  NMR. After complete consumption of the NADH model,  $H_2O$  was added and the aqueous layer was extracted with  $CH_2Cl_2$  (4 $\times$ 2 mL). The combined organic layers were dried over  $MgSO_4$  and the solvent was evaporated under reduced pressure. The crude reaction mixture was submitted to the HPLC analysis although in some cases the resulting mandelate was isolated by preparative thin layer chromatography (eluent: hexanes/EtOAc). Enantiomeric excesses were determined by HPLC using chiral stationary phases and hexanes/isopropanol as mobile phase. Reaction conditions, yields, and HPLC conditions are given in Table 2.

#### 4.8. Computational methods

All structures were optimized using the functional B3LYP<sup>24a</sup> and the 6-31G\* basis sets as implemented in Gaussian 03.<sup>25</sup> All energy minima and transition structures were characterized by frequency analysis. The energies reported in this work include zero-point vibrational energy corrections (ZPVE) and are not scaled. The stationary points were characterized by frequency calculations in order to verify that they have the right number of negative eigenvalues. The intrinsic reaction coordinates (IRC)<sup>28</sup> were followed to verify the energy profiles connecting each transition structure to the correct associated local minima. Single-point calculations with the self-consistent reaction field (SCRF) based on the IEF-PCM<sup>27</sup> solvation model (MeCN,  $\epsilon=36.64$ ) were carried out at B3LYP/6-311++G\*\* level on the previously optimized most relevant structures.

#### Acknowledgements

We thank the Ministerio de Educación y Ciencia (MEC, Spain) (Project: CTQ2006-13891/BQU), UPV-EHU and Gobierno Vasco (ETORTEK inanoGUNE IE-08/225) for financial support. Thanks are also due to SGI/IZO-SGIker for the generous allocation of computational resources and to SGIker (UPV-EHU) for NMR facilities. A grant from UPV-EHU to P.F. is acknowledged.

#### Supplementary data

NMR spectra of compounds **4a–e**, chiral HPLC chromatograms of 2-hydroxy esters **15–19**, and Cartesian coordinates of all computed

stationary points are included as Supplementary data. These data can be found in the online version, at doi:10.1016/j.tet.2010.02.085.

## References and notes

- (a) Branden, C. I.; Eklund, H. In *Dehydrogenases Requiring Nicotinamide Coenzymes*; Jeffery, J., Ed.; Birkhauser: Basel/Boston/Stuttgart, 1980; pp 40–84; (b) Branden, C. I.; Jornwall, H.; Eklund, H.; Furugren, B. In *The Enzymes*, 3rd ed; Boyer, P. D., Ed.; Academic: New York, NY, 1975; Vol. XI, pp 104–190.
- (a) Loewus, F. A.; Ofner, P.; Fisher, H. F.; Westheimer, F. H. *J. Biol. Chem.* **1953**, *202*, 699–704; (b) You, K. *Crit. Rev. Biochem.* **1984**, *17*, 313–451.
- Walsh, C. *Enzymatic Reactions Mechanisms*; Freeman, W.H.: San Francisco, 1979; pp 777–827.
- Ohnishi, Y.; Kagami, M.; Ohno, A. *J. Am. Chem. Soc.* **1975**, *97*, 4766–4768.
- For reviews on NADH models, see: (a) Inouye, Y.; Oda, N. *Asymmetric Synthesis*; Academic: New York, 1983; Vol. 2, pp 91–124; (b) Yasui, S.; Ohno, A. *Bioorg. Chem.* **1986**, *14*, 70–96; (c) Burgess, V. A.; Davies, S. G.; Skerlj, R. T. *Tetrahedron: Asymmetry* **1991**, *2*, 299–328; (d) Dupas, G.; Levacher, V.; Bourguignon, J.; Quéguiner, G. *Heterocycles* **1994**, *39*, 405–429; (e) Wang, N. X.; Zhao, J. *Synlett* **2007**, 2785–2791.
- (a) Ohno, A.; Ikeguchi, M.; Kimura, T.; Oka, S. *J. Am. Chem. Soc.* **1979**, *101*, 7036–7040; (b) Mikata, Y.; Hayashi, K.; Mizukami, K.; Matsumoto, S.; Yano, S.; Yamazaki, N.; Ohno, A. *Tetrahedron Lett.* **2000**, *41*, 1035–1038; (c) Ohno, A.; Kashiwagi, M.; Ishihara, Y. *Tetrahedron* **1986**, *42*, 961–973; (d) de Kok, P. M. T.; Bastiaansen, L. A. M.; van Lier, P. M.; Vekemans, J. A.; Buck, H. M. *J. Org. Chem.* **1989**, *54*, 1313–1320; (e) Meyers, A. I.; Oppenlaender, T. J. *J. Am. Chem. Soc.* **1986**, *108*, 1989–1996; (f) Meyers, A. I.; Brown, J. D. *J. Am. Chem. Soc.* **1987**, *109*, 3155–3156.
- (a) Burgess, V. A.; Davies, S. G.; Skerlj, R. T. *J. Chem. Soc., Chem. Commun.* **1990**, 1759–1762; (b) Burgess, V. A.; Davies, S. G.; Skerlj, R. T.; Whittaker, M. *Tetrahedron: Asymmetry* **1992**, *3*, 871–901; (c) Davies, S. G.; Skerlj, R. T.; Whittaker, M. *Tetrahedron: Asymmetry* **1990**, *1*, 725–728.
- (a) Seki, M.; Baba, N.; Oda, J.; Inouye, Y. *J. Am. Chem. Soc.* **1981**, *103*, 4613–4615; (b) Hoshida, F.; Ohi, S.; Baba, N.; Oda, J.; Inouye, Y. *Org. Chem.* **1982**, *46*, 2173–2175; (c) Seki, M.; Baba, N.; Oda, J.; Inouye, Y. *J. Org. Chem.* **1983**, *48*, 1370–1373; (d) Skog, K.; Wennerström, O. *Tetrahedron Lett.* **1992**, *33*, 1751–1754.
- (a) de Vries, J. G.; Kellogg, R. M. *J. Am. Chem. Soc.* **1979**, *101*, 2759–2761; (b) Jouin, P.; Troostwijk, C. B.; Kellogg, R. M. *J. Am. Chem. Soc.* **1981**, *103*, 2091–2093; (c) Talma, A. G.; Jouin, P.; De Vries, J. G.; Troostwijk, C. B.; Werumeus Buning, G. H.; Waninge, J.; Visscher, J.; Kellogg, R. M. *J. Am. Chem. Soc.* **1985**, *107*, 3981–3997.
- (a) Imanishi, T.; Hamano, Y.; Yoshikawa, H.; Iwata, C. *J. Chem. Soc., Chem. Commun.* **1988**, 473–475; (b) Obika, S.; Nishiyama, T.; Tatematsu, S.; Miyashita, K.; Iwata, C.; Imanishi, T. *Tetrahedron* **1997**, *53*, 593–602; (c) Obika, S.; Nishiyama, T.; Tatematsu, S.; Miyashita, K.; Imanishi, T. *Chem. Lett.* **1996**, *25*, 853–854; (d) Obika, S.; Nishiyama, T.; Tatematsu, S.; Miyashita, K.; Imanishi, T. *Tetrahedron* **1997**, *53*, 3073–3082; (e) Obika, S.; Nishiyama, T.; Tatematsu, S.; Nishimoto, M.; Miyashita, K.; Imanishi, T. *Heterocycles* **1998**, *49*, 261–267.
- (a) Ohno, A.; Ushida, S. *Mechanistic Models of Asymmetric Reductions*; Springer: Heidelberg, 1986; (b) Gase, R. A.; Pandit, U. K. *J. Am. Chem. Soc.* **1979**, *101*, 7059–7064; (c) Ohno, A.; Kimura, T.; Yamamoto, H.; Kim, S. G.; Oka, S.; Ohnishi, Y. *Bull. Chem. Soc. Jpn* **1977**, *50*, 1535–1538; (d) Ohno, A.; Yamamoto, H.; Okamoto, T.; Oka, S.; Ohnishi, Y. *Bull. Chem. Soc. Jpn* **1977**, *50*, 2385–2386.
- (a) Endo, T.; Hayashi, Y.; Okawara, M. *Chem. Lett.* **1977**, *6*, 391–394; (b) Endo, T.; Kawasaki, H.; Okawara, M. *Tetrahedron Lett.* **1979**, *20*, 23–26; (c) Katoh, A.; Naruse, S.; Ohkanda, J.; Yamamoto, H. *Heterocycles* **1997**, *45*, 1441–1446; (d) Baba, N.; Oda, J.; Inouye, Y. *J. Chem. Soc., Chem. Commun.* **1980**, 815–817; (e) Baba, N.; Amano, M.; Oda, J.; Inouye, Y. *J. Am. Chem. Soc.* **1984**, *106*, 1481–1486; (f) Makino, T.; Nunozawa, T.; Baba, N.; Oda, J.; Inouye, Y. *Tetrahedron Lett.* **1979**, *20*, 1683–1686.
- Saito, R.; Naruse, S.; Takano, K.; Fukuda, K.; Katoh, A.; Inoue, Y. *Org. Lett.* **2006**, *8*, 2067–2070.
- Aizpurua, J. M.; Palomo, C.; Fratila, R. M.; Ferron, P.; Benito, A.; Gomez-Bengoa, E.; Miranda, J. I.; Santos, J. I. *J. Org. Chem.* **2009**, *74*, 6691–6702.
- (a) Freidinger, R. M.; Veber, D. F.; Perlow, D. S.; Brooks, J. R.; Saperstein, R. *Science* **1980**, *210*, 656–658; (b) Freidinger, R. M.; Schwenk, D.; Veber, D. F. *J. Org. Chem.* **1982**, *47*, 104–109; (c) Freidinger, R. M. *J. Org. Chem.* **1985**, *50*, 3631–3633; (d) Freidinger, R. M. *J. Med. Chem.* **2003**, *46*, 5553–5566.
- (a) Palomo, C.; Aizpurua, J. M.; Benito, A.; Galarza, R.; Khamrai, U. K.; Vazquez, J.; DePascual-Teresa, B.; Nieto, P. M.; Linden, A. *Angew. Chem., Int. Ed.* **1999**, *38*, 3056–3058; (b) Palomo, C.; Aizpurua, J. M.; Benito, A.; Miranda, J. I.; Fratila, R. M.; Matute, C.; Domercq, C. M.; Gago, F.; Martin-Santamaria, S.; Linden, A. *J. Am. Chem. Soc.* **2003**, *125*, 16243–16260.
- Ohno, A.; Ikeguchi, M.; Kimura, T.; Oka, S. *J. Chem. Soc., Chem. Commun.* **1978**, 328–329.
- (a) Palomo, C.; Aizpurua, J. M.; Legido, M.; Galarza, R.; Deya, P. M.; Dunogues, J.; Picard, J. P.; Ricci, A.; Seconi, G. *Angew. Chem., Int. Ed.* **1996**, *35*, 1239–1241; (b) Palomo, C.; Aizpurua, J. M.; Legido, M.; Mielgo, A.; Galarza, R. *Chem.—Eur. J.* **1997**, *3*, 1432–1441; (c) Palomo, C.; Aizpurua, J. M.; Ganboa, I.; Benito, A.; Cuervo, L.; Fratila, R. M.; Jimenez, A.; Loinaz, I.; Miranda, J. I.; Pytlewska, K. R.; Micle, A.; Linden, A. *Org. Lett.* **2004**, *6*, 4443–4446.
- Palomo, C.; Aizpurua, J. M.; Balentova, E.; Jimenez, A.; Oyarbide, J.; Fratila, R. M.; Miranda, J. I. *Org. Lett.* **2007**, *9*, 101–104.
- (a) Seebach, D.; Aebi, J. D. *Tetrahedron Lett.* **1984**, *25*, 2545–2548; (b) Seebach, D.; Aebi, J. D.; Gander-Coquoz, M.; Naef, R. *Helv. Chim. Acta* **1987**, *70*, 1194–1216.
- Vicario, J. L.; Badía, D.; Carrillo, L. *J. Org. Chem.* **2001**, *66*, 9030–9032.
- Kanomata, N.; Nakata, T. *J. Am. Chem. Soc.* **2000**, *122*, 4563–4568.
- Li, J.; Liu, Y.; Deng, J. G.; Li, X.; Cui, X.; Li, Z. *Tetrahedron: Asymmetry* **2000**, *11*, 2677–2682.
- (a) Lee, C.; Yang, W.; Parr, R. G. *Phys. Rev. B* **1988**, *37*, 785–789; (b) Becke, A. D. *J. Chem. Phys.* **1993**, *98*, 5648–5652; (c) Kohn, W.; Becke, A. D.; Parr, R. G. *J. Phys. Chem.* **1996**, *100*, 12974–12980.
- Frisch, M. J.; Trucks, G. W.; Schlegel, H. B.; Scuseria, G. E.; Robb, M. A.; Cheeseman, J. R.; Montgomery, J. A., Jr.; Vreven, T.; Kudin, K. N.; Burant, J. C.; Millam, J. M.; Iyengar, S. S.; Tomasi, J.; Barone, V.; Mennucci, B.; Cossi, M.; Scalmani, G.; Rega, N.; Petersson, G. A.; Nakatsuji, H.; Hada, M.; Ehara, M.; Toyota, K.; Fukuda, R.; Hasegawa, J.; Ishida, M.; Nakajima, T.; Honda, Y.; Kitao, O.; Nakai, H.; Klene, M.; Li, X.; Knox, J. E.; Hratchian, H. P.; Cross, J. B.; Bakken, V.; Adamo, C.; Jaramillo, J.; Gomperts, R.; Stratmann, R. E.; Yazyev, O.; Austin, A. J.; Cammi, R.; Pomelli, C.; Ochterski, J. W.; Ayala, P. Y.; Morokuma, K.; Voth, G. A.; Salvador, P.; Dannenberg, J. J.; Zakrzewski, V. G.; Dapprich, S.; Daniels, A. D.; Strain, M. C.; Farkas, O.; Malick, D. K.; Rabuck, A. D.; Raghavachari, K.; Foresman, J. B.; Ortiz, J. V.; Cui, Q.; Baboul, A. G.; Clifford, S.; Cioslowski, J.; Stefanov, B. B.; Liu, G.; Liashenko, A.; Piskorz, P.; Komaromi, I.; Martin, R. L.; Fox, D. J.; Keith, T.; Al-Laham, M. A.; Peng, C. Y.; Nanayakkara, A.; Challacombe, M.; Gill, P. M. W.; Johnson, B.; Chen, W.; Wong, M. W.; Gonzalez, C.; Pople, J. A. *Gaussian 03, Revision D.03*; Gaussian: Wallingford, CT, 2004.
- (a) Kluge, S.; Weston, J. *Biochemistry* **2005**, *44*, 4877–4885; (b) Cha, J.-N.; Cheong, B.-S.; Cho, H.-G. *J. Phys. Chem. A* **2001**, *105*, 1789–1796.
- (a) Cancès, E.; Mennucci, B.; Tomasi, J. *J. Chem. Phys.* **1997**, *107*, 3032–3047; (b) Cossi, M.; Barone, V.; Mennucci, B.; Tomasi, J. *J. Chem. Phys. Lett.* **1998**, *286*, 253–260; (c) Tomasi, J.; Mennucci, B.; Cancès, E. *J. Mol. Struct. (Theochem)* **1999**, *466*, 211–226.
- Gonzalez, C.; Schlegel, H. B. *J. Phys. Chem.* **1990**, *94*, 5523–5527.